JOURNAL OF MATERIALS SCIENCE **37** (2002) 1273–1279

Fabrication of new porcelain body using nonplastic raw materials by slip casting

WEON-PIL TAI
Institute of Advanced Materials, Inha University, Yonghyun-Dong, Nam-ku, Inchon 402-751, Korea
E-mail: wptai@munhak.inha.ac.kr

K. KIMURA
Inorganic Materials Department, Kyushu National Industrial Research Institute, Tosu, Saga 841-0052, Japan

K. JINNAI
Advanced Science and Technology Center for Cooperative Research, Kyushu University, Kasuga, Fukuoka 810-8580, Japan

New porcelain bodies using only nonplastic raw materials, such as volcanic glass, quartz, alumina and aluminous cement, were fabricated, and their properties were investigated. Green strength increased with increasing Al_2O_3 content at the constant amount of volcanic glass and aluminous cement, caused by the increase of green bulk density with small sized Al_2O_3 addition. The phases in the fired body were glass, α-quartz, cristobalite, anorthite and α-Al_2O_3. High flexural strength with 10 wt% Al_2O_3 addition was attributed to a strong residual stress induced by the large difference in the thermal expansion coefficient between the glass matrix and the quartz grains, and an additional prestress was induced by Al_2O_3 grains. Higher density and fewer fracture origin were also indicated as potential factors leading to the strengthening effect.

1. Introduction

Slip casting is a suitable consolidation process to obtain materials with high green density and microstructural homogeneity allowing the manufacture of components with complex shapes [1]. The slip casting has been used for many years in the production of conventional ceramics. The development of fine ceramics by this method also has gained in importance during recent years [2, 3].

Most porcelains are feldspathic porcelains made by slip casting using feldspar, quartz, and clay minerials [4, 5], but the deposits of high-grade plastic raw materials have recently started to exhaust. Thus, a new approach to the development of porcelain bodies without using plastic raw materials is necessary. Plastic raw materials are normally required because they provide plasticity for forming, and transform into glass and crystalline phases during firing. In the present study, the plastic raw materials have been replaced by an aluminous cement (calcium aluminate cement). The aluminous cement can increase the green strength by the hydration reaction in moist atmospheres without using any binder and plastic raw materials [6, 7]. It also melts with volcanic glass and quartz during the firing process, and the melted glass phase is crystallized to anorthite ($CaO \cdot Al_2O_3 \cdot 2SiO_2$) [8]. Borglum *et al.* [9] synthesized a hexagonal anorthite by hydrothermal processing of monocalcium aluminate and quartz at low temperature. Quartz acts as a skeleton in the fired body. Volcanic glass plays the role of a flux such as feldspar and consists of glass matrix in the fired body. To develop a new porcelain body that possesses high-strength, the quartz skeleton in the fired body should be kept to some degree under better vitrification during the firing process. Moreover, the prestress for increasing the strength of the fired body should be generated by the large difference in the thermal expansion coefficient between the glass phase and the quartz grains [10, 11]. Alumina [12, 13], cristobalite [14] and mullite [15, 16] in the fired body were also acted as potential factors leading to the strengthening effect.

In the present study, new porcelain bodies, which exhibit lightweight and high-strength, are fabricated by addition of alumina to only nonplastic raw materials, such as volcanic glass, quartz and aluminous cement, without using a binder. The properties of those resultant bodies were investigated.

2. Experimental procedure

2.1. Raw materials

The starting raw materials were 1.6 μm volcanic glass powder, 0.2 μm Al_2O_3 powder (AKP-53, Sumitomo Chemical Co., Japan), 4.6 μm silica stone powder, quartz (Ube industries, LTD., Japan), and aluminous cement powder (Ube industries, LTD., Japan) with an average particle size of 14.5 μm. The powders were mixed in the ranges of 5–20 wt% Al_2O_3, 10–30 wt%

TABLE I Chemical compositions of raw materials (wt%)

	SiO_2	Al_2O_3	Fe_2O_3	TiO_2	CaO	MgO	Na_2O	K_2O	Ig.loss	Total
Volcanic glass	74.79	11.56	1.78	0.11	0.80	0.37	2.22	2.12	5.67	99.42
Silica stone	98.10	1.00	0.20							99.30
Aluminous cement	0.55	70.38	0.14		28.13	0.20				99.40
Alumina		99.99								99.99

quartz, and constant amount of volcanic glass (50 wt%) and aluminous cement (20 wt%). Volcanic glass particle was separated by elutriation method to obtain a smaller particle size. The chemical compositions of the raw materials are shown in Table I. Silica stone consisted of quartz, designated as quartz. Aluminous cement consisted of $CaAl_2O_4$ and $CaAl_4O_7$.

2.2. Sample preparation

The composition of 50 wt% volcanic glass, 30 wt% quartz and 20 wt% aluminous cement was chosen as the base composition. Al_2O_3 was added to select the optimum particle size distribution for slip casting and it was substitutionally added for quartz. Slips were prepared to obtain the optimum particle size distribution, deflocculant content and distilled water content for slip casting. The powder mixtures added only distilled water and deflocculant were stirred with 250 rpm for 1 h in a stirrer for preparing aqueous slips. Water glass was added as a deflocculant (dispersant) to obtain well-dispersed concentrated aqueous slips. 0.5 wt% water glass aqueous solution was added with 56 wt%. Slips were casted in a cylindrical plaster mold into cylindrical bars of 10.5 mm $\Phi \times 81$ mm dimensions. The consolidated cylindrical bars were removed from the mold after 30 min. Hydration time of the consolidated specimens was aged for 24 h at room temperature in moist atmosphere and then the specimens were dried in an oven for 24 h at 50°C. The firing was performed in a electric furnace for 2 h at 1300°C. The heating rate was 10°C/min in temperature ranges 25–1000°C and 5°C/min in temperature range of 1000–1300°C. The cooling rate was 10°C/min.

2.3. Measurements and analyses

The size of volcanic glass, quartz and Al_2O_3 particle were measured by Microscan II (Quanta Chrome Co., USA). Particle size of aluminous cement was measured by Microtrac (Leeds & Northrup Co., USA). The bulk density of green body was calculated using the weight and volume. The bulk density of the fired body was determined by water immersion, based on ASTM C20. Rheological measurement was performed with a rotational controlled stress Rheometer (KEIKI Co., Ltd., Tokyo), immediately after the slip conditioning at a constant temperature of 20°C. The measuring configuration was a concentric coaxial cylinder and both steady shear and stress sweep measurement was conducted in the shear rate range 3.8 to 383 s^{-1}. For the interplanar spacing analyses, the fired bodies were ground by a SiC abrasive paper and then followed by polishing with diamond paste (1 and 3 μm) and lapping oil. X-ray diffraction (XRD, Philips, Holland) analyses were conducted using Cu K_α radiation to determine interplanar spacing of the quartz (112) plane and the Al_2O_3 (116) plane in the fired bodies. As a standard, the interplanar spacing of (112) plane and (116) plane of quartz and Al_2O_3 powder was conducted. XRD analyses were also conducted to determine the phases. Fracture surfaces were observed by scanning electron microscopy (SEM, ABT, Japan). Linear shrinkage was measured on the length direction before and after the firing. Water absorption was measured based on JIS-R2205. The flexural strength was measured by three-point bending test (Shimadzu, AGS-5KND, Japan) with a lower span of 30 mm under a crosshead speed of 0.5 mm/min, based on JIS-R1601. The surface condition of measured samples in the green body and fired body was as-dried and as-fired condition, respectively. Sample number used was more than five.

3. Results and discussion

3.1. Preparation of green bodies by slip casting

Fig. 1 shows particle size distributions along with the substitutional addition of submicron-sized Al_2O_3 powder for quartz for preparing the green body by slip casting without using any binders and plastic raw materials. The base composition is 50 wt% volcanic glass, 30 wt% quartz and 20 wt% aluminous cement. A standard particle size distribution in Arita, Japan porcelain industry for slip casting is also shown in Fig. 1. The addition of 5 wt% Al_2O_3 indicates 5 wt% Al_2O_3, 25 wt% quartz, and constant amount of volcanic glass (50 wt%) and aluminous cement (20 wt%) in the percentages. In particular, the particle size of below 1 μm is increased by

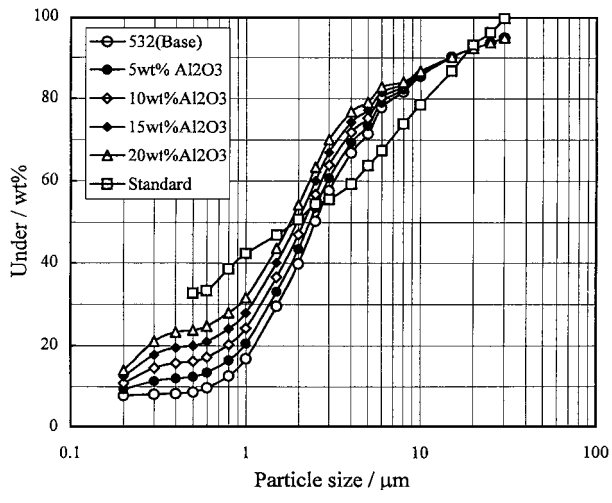

Figure 1 Particle size distributions with Al_2O_3 addition for slip casting under constant volcanic glass (50 wt%) and aluminous cement (20 wt%).

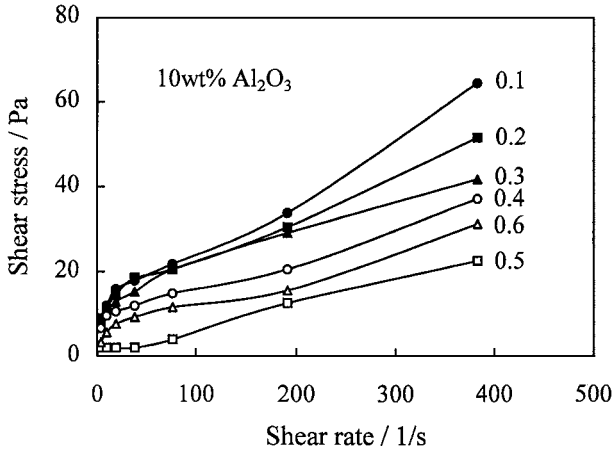

Figure 2 Relation of shear stress and shear strain of the suspensions with 10 wt% Al_2O_3 addition at different water glass contents.

Al_2O_3 addition, nearing to a standard particle distribution. The addition of larger amount of Al_2O_3 is more well slip casted, leading to higher green strength as explains latter.

Fig. 2 shows relation of shear stress and shear strain of the suspensions with 10 wt% Al_2O_3 addition at various water glass contents. It makes possible to compare the influence of the dispersant (deflocculant) upon the rheological behavior. The shear stress decreases with adding the dispersant up to 0.5 wt% water glass content and then increases with a higher water glass content. The decrease of the shear stress with water glass content of up to 0.5 wt% means the shift of flocculation to dispersion state. The apparent viscosity at the dispersion state having 0.5 wt% water glass content exhibits a minimum value, as shown in Fig. 3. The lowest apparent viscosity indicates that the repulsive force inhibits agglomeration between the suspended particles.

Fig. 4 shows X-ray diffraction pattern of the green body with 10 wt% Al_2O_3 content that keep for 24 h in a moist atmosphere. The phases formed in the green body with the hydration time of 24 h are α-quartz, α-Al_2O_3 and $CaAl_4O_7$, and a small amount of $(Ca, Na)_{1.3}(Si, Al)_9O_{18} \cdot 8H_2O$, leading to a maximum green strength due to hardening by a hydration reaction. It is remarkable that $CaAl_2O_4$ phase, one phase of aluminous cement, disappears during the hydration time of 24 h. In the glass microspheres-quartz-aluminous cement system [7], the flexural strength of green body (green strength) also attained to a maximum value at hydration time of 24 h in moist atmospheres. All the green bodies thereafter are kept for hydration time of 24 h that exhibits a maximum value in green strength.

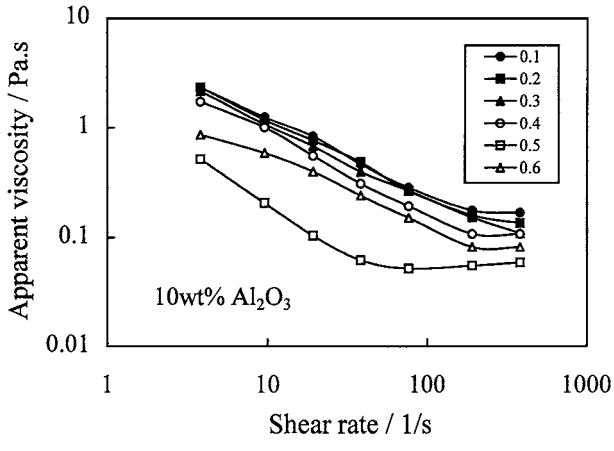

Figure 3 Effect of water glass content on apparent viscosity of the suspensions with 10 wt% Al_2O_3 addition.

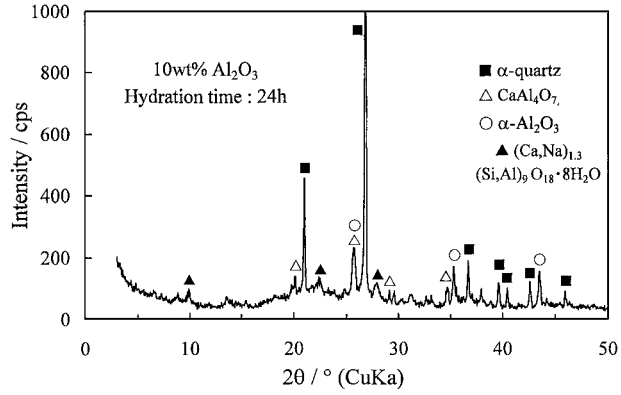

Figure 4 X-ray diffraction pattern in the green body with 10 wt% Al_2O_3 content and hydration time of 24 h.

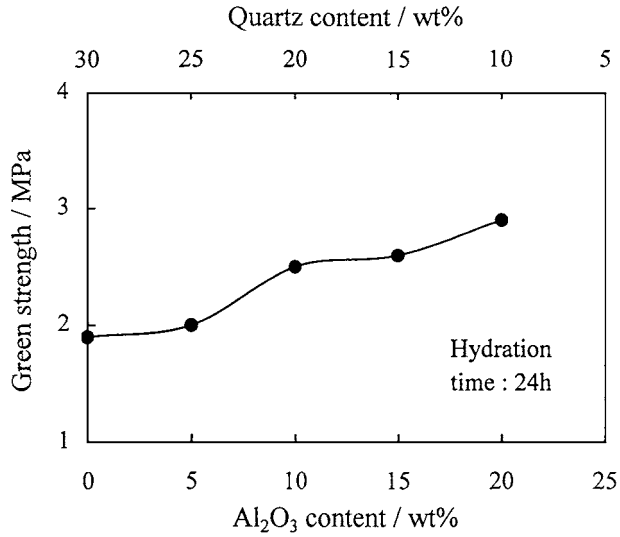

Figure 5 Variation of green strength as a function of Al_2O_3 content in the green bodies.

Fig. 5 shows change of green strength as a function of Al_2O_3 content in the system of volcanic glass-alumina-quartz-aluminous cement. The green strength increases slightly with Al_2O_3 addition of up to 5 wt% and then increases remarkedly with the addition of higher Al_2O_3 content at constant amount of volcanic glass and aluminous cement. This indicates that the addition of larger amount of submicron-sized Al_2O_3 compacts the green body by a more easy slip casting. Fig. 6 shows change of bulk density with Al_2O_3 content in the green body. The variation of bulk density shows similar tendency to that of the green strength. The addition of submicron-sized Al_2O_3 is more well slip casted, leading to denser green body. The bulk density with increasing the content of Al_2O_3 is increased by the formation of denser body due to the increase of submicron-sized Al_2O_3 particles in the mixtures as shown in Fig. 1. The increased green strength with increasing Al_2O_3 content thus is

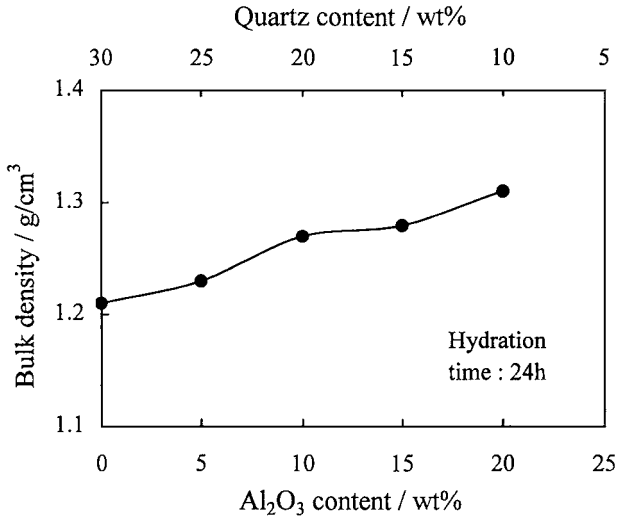

Figure 6 Change in bulk density as a function of Al_2O_3 content in the green bodies.

attributed to the increase of green bulk density due to the increase of small sized Al_2O_3 particles.

3.2. Fabrication of sintered bodies

Fig. 7 shows X-ray diffraction patterns with Al_2O_3 content in the fired bodies at 1300°C for 2 h. The firing temperature is fixed at 1300°C because the composition of glaze and underglaze decoration is based on the temperature of 1300°C. The phases formed at almost all the fired bodies are glass, α-quartz, α-cristobalite, anorthite and α-Al_2O_3. α-Al_2O_3 peak increases markedly with increasing the content of Al_2O_3. The Al_2O_3 may

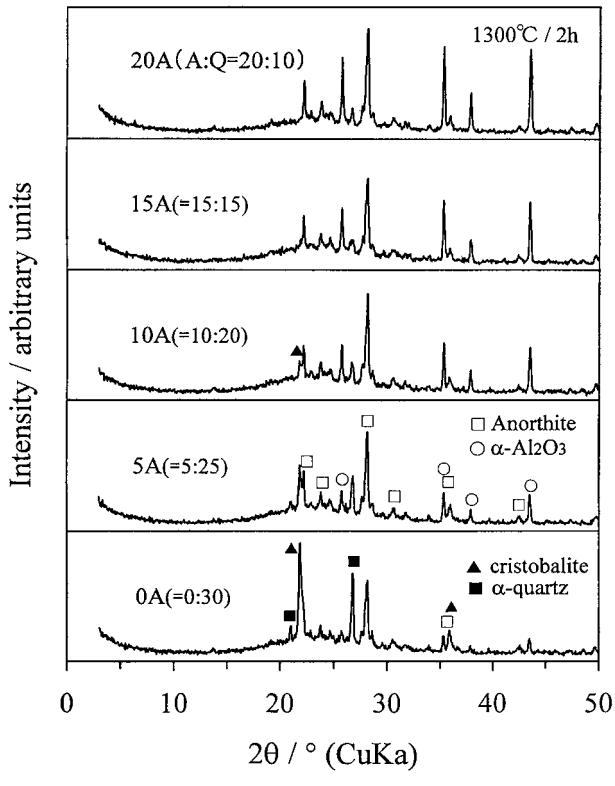

Figure 7 X-ray diffraction patterns with Al_2O_3 addition in the fired bodies under constant volcanic glass (50 wt%) and aluminous cement (20 wt%). A, Al_2O_3; Q, Quartz.

be partly reacted with the other components at the temperature of 1300°C. However, the addition of above 15 wt% Al_2O_3 should be fired at higher temperature to produce denser body and higher strength, as explains latter. Anorthite peak is almost constant with increasing Al_2O_3 content at constant amount of volcanic glass (50 wt%) and aluminous cement (20 wt%). The $CaAl_4O_7$ phase, aluminous cement component, kept during the hydration time of above 24 h in the green body disappears during the firing process. These imply that anorthite is formed by the crystallization from the glassy phase melted from volcanic glass, quartz and aluminous cement [8], and partly Al_2O_3 during the firing process. Kobayashi and Kato [17] synthesized anorthite from kaolin and $CaCO_3$. The peak of α-quartz decreases with increasing Al_2O_3 content, i.e., less quartz content. Cristobalite peak decreases with the increased Al_2O_3 content and, finally, the cristobalite does not form at a 20 wt% Al_2O_3 addition. That is, α-quartz and cristobalite peaks are decreased by the replacement addition of some of the quartz by Al_2O_3. The viscosity of volcanic glass is quite rapidly decreased at about 1100°C and the decreased viscosity of glass phase with a large amount of volcanic glass makes quartz particles melt easily. The higher Al_2O_3 content lowers the amount of liquid phase [18], leading to the increase of densification temperature. Lundin [19] suggested that the amorphous silica liberated during the decomposition of metakaolin transformed directly to cristobalite at about 1050°C. Carty and Senapati [14] argued that cristobalite was formed either from the glass phase or by the direct conversion of quartz. In the present study, cristobalite peak decreases notably with increasing Al_2O_3 content, and the cristobalite disappears at addition of 20 wt% Al_2O_3. On the other hand, the addition of higher quartz content, smaller amount of Al_2O_3, possesses higher SiO_2 content in the glass phase dissolved from quartz particles because the highly siliceous glass is formed from larger amount of quartz during the firing process, and the highly siliceous glass is easy to crystallize to cristobalite.

3.3. Properties of sintered bodies

Fig. 8 shows change in flexural strength with Al_2O_3 content in the fired bodies. The flexural strength of the fired body increases with increasing Al_2O_3 content, attaining a maximum value at 10 wt% Al_2O_3 addition, and then decreases with the addition of any more Al_2O_3. The higher Al_2O_3 content lowers the flexural strength at a constant firing temperature, even though the addition of larger amount of Al_2O_3 is more well slip casted and exhibits higher green strength. It is necessary to firing at higher temperature to be vitrified the mixture having a larger amount of Al_2O_3. The addition of larger amount of aluminous cement was also necessary for higher flexural strength to firing at higher temperature [7]. The Al_2O_3 addition of up to 10 wt% produces bodies which are sintered and vitrified well. The addition of 10 wt% Al_2O_3 leads to better vitrification under firing for 2 h at 1300°C.

Fig. 9 shows change in bulk density with Al_2O_3 content in the fired bodies. The bulk density exhibits a

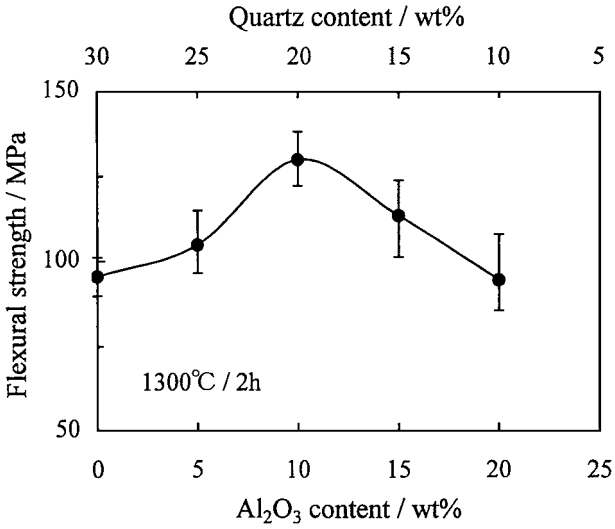

Figure 8 Variation of flexural strength as a function of Al_2O_3 content in the fired bodies. Error bars show the minimum and maximum values observed.

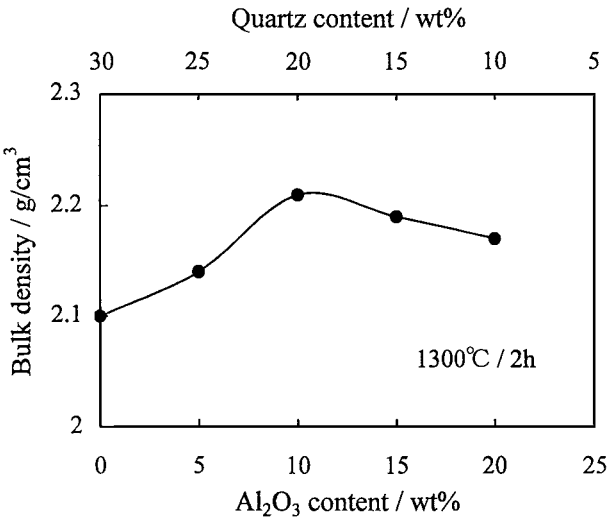

Figure 9 Change in bulk density as a function of Al_2O_3 content in the fired bodies.

maximum value with the addition of 10 wt% Al_2O_3, and then the density decreases with higher Al_2O_3 content. The addition of aluminous cement as a substitute for plastic raw material forms anorthite in all the fired bodies. The density of anorthite (2.76 g/cm^3) [20] is lower than that of mullite (3.16 g/cm^3) [21] formed in general porcelain body. In this study, the bulk density is low as between 2.10 and 2.21 g/cm^3 due to the partly under-firing and over-firing, and the formation of anorthite in all the fired bodies. The change of bulk density is almost proportional to that of flexural strength, as shown in Figs 8 and 9. The flexural strength is closely related to the water absorption, as shown in Fig. 10. This indicates that smaller water absorption generates lower stress concentration at the surface of the fired body because the body with small water absorption does not have almost surface defect. Fig. 10 shows change in water absorption with Al_2O_3 content. The water absorption is almost 0 in the range 0 wt% to 10 wt% Al_2O_3, and then the value increases with the addition of much more Al_2O_3. The small water absorption with

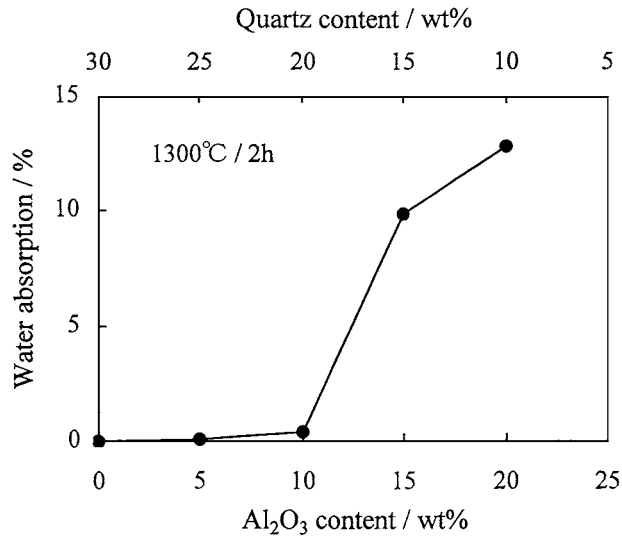

Figure 10 Water absorption with Al_2O_3 addition in the fired bodies.

Al_2O_3 additions of up to 10 wt% is attributed to easy vitrification due to the lowly viscous glass phase during the firing process at 1300°C. The large water absorption with the addition of higher Al_2O_3 content could be due to under-sintering during the firing process at all the same temperature.

Fig. 11 shows SEM micrographs of fracture surface with Al_2O_3 content. The pore size in the fired body at 10 wt% Al_2O_3 addition is relatively small by appropriate vitrification (Fig. 11c). However, the pore size in the range 0 to 5 wt% Al_2O_3 is relatively large due to a large amount of lowly viscous glass phase (Fig. 11a and b), even though the water absorption is small. On the other hand, the addition of large amount of Al_2O_3 makes the body under-sinter due to the increased viscosity of glass phase during the firing process, leading to large pores (Fig. 11d). This is demonstrated by comparing the water absorption, consisting with large water absorption at Al_2O_3 addition of above 15 wt% as shown in Fig. 10. The flexural strength of the fired body decreases because the surface at under-sintered body acts as a fracture origin. The maximum density at 10 wt% Al_2O_3 addition is attributed to the formation of denser body by better vitrification, together with appropriate Al_2O_3 addition and easy slip casting.

The addition of higher Al_2O_3 content, i.e., less quartz addition makes quartz skeleton decrease in the fired body, as shown in Fig. 7. Quartz grains generally act as a skeleton in fired body and, hence, the large decrease of the skeleton can lead to the decrease of flexural strength. Appropriate amount of quartz should be kept to generate prestress in the glass matrix by the difference in the thermal expansion coefficient between the glass phase and the quartz grains. Maity and Sarkar [22] reported that the replacement of some of the quartz by sillimanite sand increased the strength, hypothesized as a dispersion-strengthening effect. Blodgett [23] also showed the strength increase in the porcelain bodies with the addition of Al_2O_3 particles. In this study, the replacement of some of the quartz by 10 wt% Al_2O_3 increases flexural strength. On the other hand, cristobalite forms in all the mixtures except 20 wt% Al_2O_3

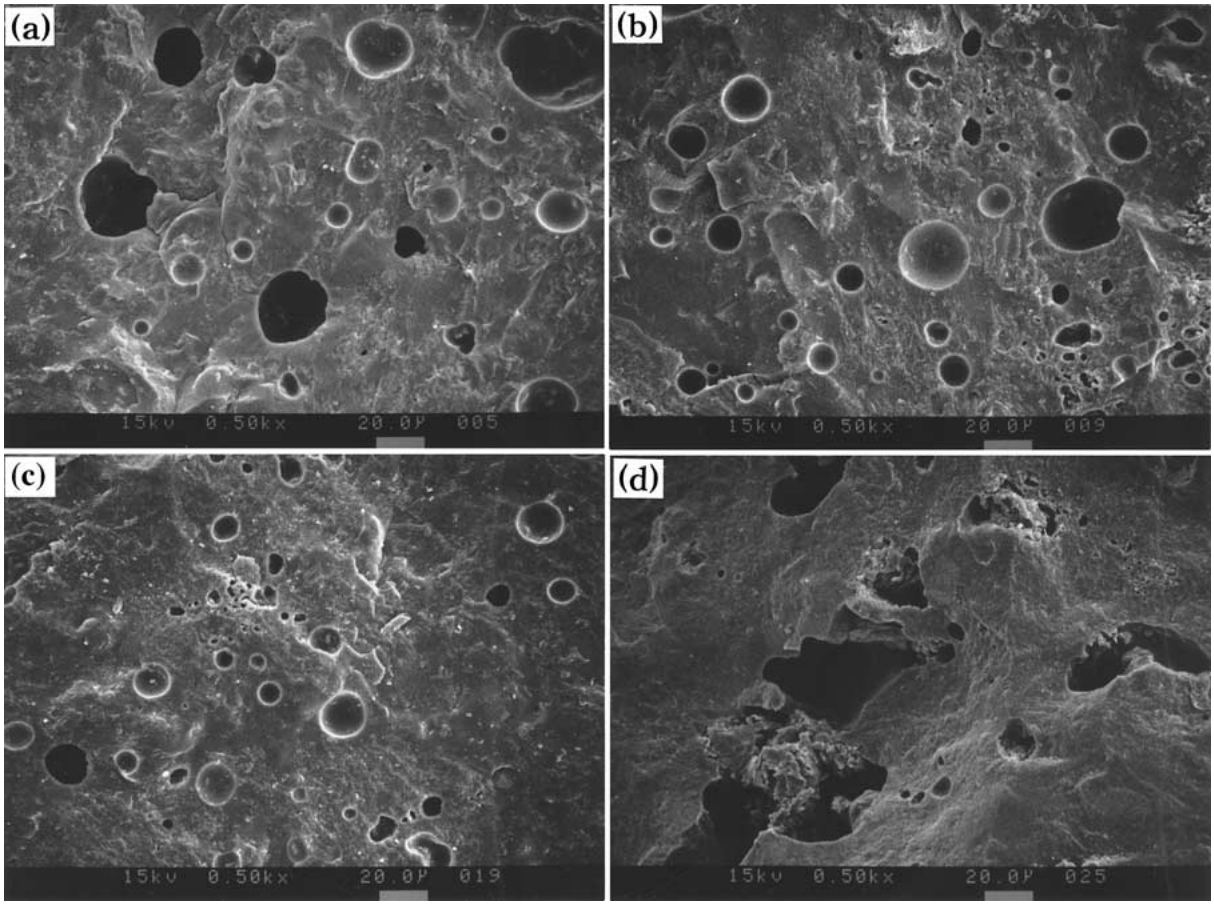

Figure 11 SEM photographs of fracture surface with Al_2O_3 addition in the fired bodies: (a) 0 wt%, (b) 5 wt%, (c) 10 wt% and (d) 20 wt% Al_2O_3.

content and the peak decreases with increasing Al_2O_3 content, decreasing quartz content. Carty and Senapati [14] have explained the increase of strength in cristobalite porcelain: the cristobalite grains are much smaller than the quartz grain and the cristobalite produces lower strain during the cooling process because the inversion temperature of cristobalite is lower than that of quartz. In the present system, the flexural strength at 10 wt% Al_2O_3 addition exhibits a maximum value, even though a larger amount of cristobalite forms at 0 wt% Al_2O_3 content, base composition. However, the strength lowers at 0 wt% Al_2O_3 content despite the formation of a larger amount of cristobalite. Cristobalite does not seem to play a major role in the improvement of flexural strength, in accordance with the present results.

For a more detailed analysis, XRD was used to investigate the cause of higher flexural strength at the addition of 10 wt% Al_2O_3. Fig. 12 shows interplanar spacing of quartz (112) plane (around $2\theta = 50.16$) with Al_2O_3 content and a standard quartz (112) plane as a dotted line. Fig. 13 also shows interplanar spacing of Al_2O_3 (116) plane (around ($2\theta = 57.6$) with Al_2O_3 content and a standard Al_2O_3 (116) plane as a dotted line. The interplanar spacing of quartz (112) plane is constant up to 10 wt% Al_2O_3 addition, then the value decreases with the addition of higher Al_2O_3 content. On the other hand, the interplanar spacing of Al_2O_3 (116) plane exhibits a maximum value at 10 wt% Al_2O_3 content. The interplanar spacing decreases with the addition of a larger amount of Al_2O_3, then the interplanar spacing in the fired body exhibits the same value as a standard Al_2O_3

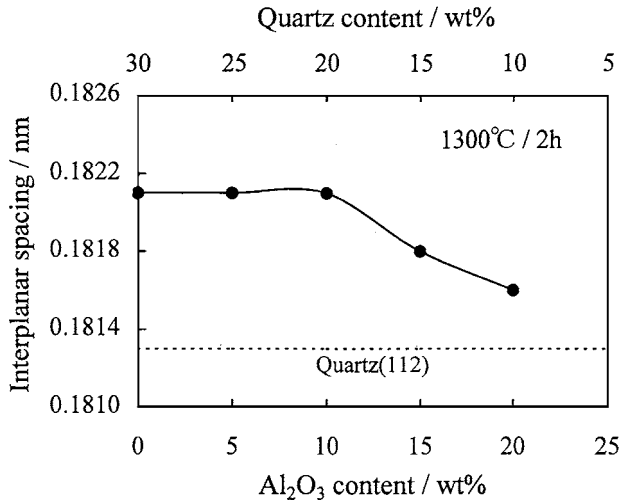

Figure 12 Interplanar spacing of quartz (112) plane with Al_2O_3 addition in the fired bodies. - - - Quartz (112) standard.

(116) plane. The larger interplanar spacings in the fired body compared to those of (112) and (116) planes of standard quartz and alumina mean the occurrence of larger residual tensile strain of the quartz and alumina grains in the fired body [24]. Hence, a strong compressive stress is produced on the glass phase surrounding the quartz grain in the fired body up to 10 wt% Al_2O_3 addition. Moreover, an additional compressive stress is produced on the glass phase surrounding the Al_2O_3 grain at 10 wt% Al_2O_3 addition, exhibiting a maximum value in the interplanar spacing of Al_2O_3 (116) plane.

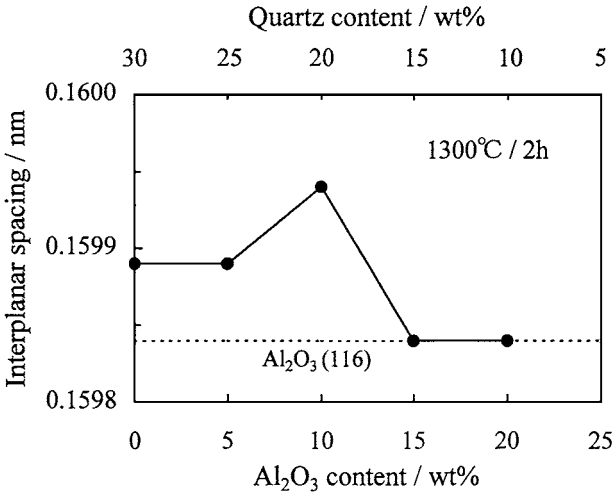

Figure 13 Interplanar spacing of Al_2O_3 (116) plane with Al_2O_3 addition in the fired bodies. - - - Al_2O_3 (116) standard.

The maximum strain of quartz and Al_2O_3 grains thus occurs at 10 wt% Al_2O_3 content, which agrees with a maximum flexural strength. The fired body that exhibits larger interplanar spacing with 10 wt% Al_2O_3 addition produces a stronger compressive stress on the dense glass phase, i.e., residual stress effect [10, 24], surrounding the quartz grains by larger difference in the thermal expansion coefficient between the glass matrix and the quartz grains during the cooling process. Also, an additional residual stress is produced by Al_2O_3 grains. Thus, high flexural strength with 10 wt% Al_2O_3 addition is attributed to stronger prestress effect, fewer fracture origins and higher density in the fired body due to better vitrification.

The linear shrinkage decreases (18.5 to 16.9%) slightly with increasing Al_2O_3 content up to 10 wt% Al_2O_3 addition but it decreases (14.9 to 13.9%) largely with higher Al_2O_3 content, from 15 to 20 wt%. This indicates that the addition of much more Al_2O_3 is not vitrified easily by glass phase at 1300°C.

4. Conclusions

New porcelain bodies which possess lightweight and high-strength were fabricated using only nonplastic raw materials and their properties were investigated. Green strength increases with increasing Al_2O_3 content and the increased strength is attributed to the increase of the green bulk density by a more easy slip casting, caused by the increase of submicron-sized Al_2O_3 content. The phases formed in the fired body are glass, α-quartz, cristobalite, anorthite and α-Al_2O_3. α-Al_2O_3 peak increases with increasing Al_2O_3 content, which may not almost react with the glass phase at 1300°C. Anorthite peak is almost constant with increasing Al_2O_3 content. Cristobalite decreases in intensity as increasing Al_2O_3 content and disappears at 20 wt% Al_2O_3 addition. High flexural strength (130 MPa) with 10 wt% Al_2O_3 addition is attributed to stronger prestress, higher density and fewer fracture origins in the fired body due to better vitrification. The bulk density in the fired body is low as 2.10 to 2.21 g/cm^3. Porcelains which exhibit lightweight and high-strength can be produced by slip casting using only nonplastic raw materials and deflocculant.

References

1. C. OLAGNON, D. Mc. GARRY and E. NAGY, *Br. Ceram. Trans. J.* **88** (1989) 75.
2. N. MIZUTANI, T. OGIHARA, M. KONDO, M. IKEDA and K. SHINOZAKI, *J. Mater. Sci.* **29** (1994) 366.
3. M. P. ALBANO and L. B. GARRIDO, *J. Amer. Ceram. Soc.* **81** (1998) 837.
4. K. HAMANO, Y. H. WU, Z. NAKAGAWA and M. HASEGAWA, *J. Ceram. Soc. Jpn.* **99** (1991) 1110.
5. N. SUGIYAMA, R. HARADA and H. ISHIDA, *ibid.* **104** (1996) 312.
6. K. MISHIMA, "Seramikku Kogaku Handobukku" (Ceramic Engineering Handbook) (Ceramic Society of Japan, Gihodo Shuppan, 1989) p. 1105 [in Japanese].
7. W. P. TAI, K. KIMURA, H. TATEYAMA, N. YAMADA and K. JINNAI, *J. Ceram. Soc. Jpn.* **107** (1999).
8. E. M. LEVIN, C. R. ROBBINS and H. F. MCMURDIE, "Phase Diagrams for Ceramists," Vol. 1 (American Ceramic Society, Columbus, OH, 1964) Fig. 630.
9. B. P. BORGLUM, J. M. BUKOWSKI, J. F. YOUNG and R. C. BUCHANAN, *J. Amer. Ceram. Soc.* **76** (1993) 1354.
10. L. MATTYASOVSZKY-ZSOLNAY, *ibid.* **40** (1957) 299.
11. K. HAMANO and M. HIRAYAMA, *J. Ceram. Soc. Jpn.* **102** (1994) 665.
12. C. R. AUSTIN, H. Z. SCHOFIELD and N. L. HALDY, *J. Amer. Ceram. Soc.* **29** (1946) 341.
13. R. HARADA, N. SUGIYAMA and H. ISHIDA, *Ceram. Eng. Sci. Proc.* **17** (1996) 88.
14. W. M. CARTY and U. SENAPATI, *J. Amer. Ceram. Soc.* **81** (1998) 3.
15. S. J. MCDOWELL and E. J. VACHUSKA, *ibid.* **10** (1927) 64.
16. S. C. SANE and R. L. COOK, *ibid.* **34** (1951) 145.
17. Y. KOBAYASHI and E. KATO, *ibid.* **77** (1994) 833.
18. N. SUGIYAMA, R. HARADA and H. ISHIDA, *J. Ceram. Soc. Jpn.* **105** (1997) 126.
19. S. T. LUNDIN, "Microstructure of Ceramic Materials" Vol. 257 (NBS Misc. Publ., 1964) p. 93.
20. W. F. COLE, H. SORUM and W. H. TAYLOR, *Acta Crystallog.* **4** (1951) 20.
21. "CRC Handbook of Chemistry and Physics," 74th ed., edited by D. R. Lide and H. P. R. Frederikse (Boca Raton, FL, 1993) pp. 4–37.
22. S. MAITY and B. K. SARKAR, *J. Eur. Ceram. Soc.* **16** (1996) 1083.
23. W. E. BIODGETT, *Am. Ceram. Soc. Bull.* **40** (1961) 74.
24. K. HAMANO, Y. H. WU, Z. NAKAGAWA and M. HASEGAWA, *J. Ceram. Soc. Jpn.* **99** (1991) 153.

Received 20 April 2000
and accepted 14 May 2001